Dual Quaternion Synthesis of Constrained Robotic Systems

Alba Perez
e-mail: maperez@uci.edu

J. M. McCarthy
Robotics and Automation Laboratory,
Dept. of Mechanical and Aerospace Engineering,
University of California,
Irvine, California 92697
e-mail: jmmccart@uci.edu

This paper presents a dual quaternion methodology for the kinematic synthesis of constrained robotic systems. These systems are constructed from one or more serial chains such that each chain imposes at least one constraint on the movement of the workpiece. Serial chains that have constrained workspaces can be synthesized by evaluating the kinematics equations of the chain on a finite set of task positions. In this case, the end-effector positions are known and the Denavit-Hartenberg parameters become design variables. Here we reformulate the kinematics equations in terms of successive screw displacements so the design variables are the coordinates defining the joint axes of the chain in a reference position. Then, dual quaternions defining these transformations are introduced to simplify the structure of the design equations. The result is a synthesis formulation that can be applied to a broad range of constrained serial chains, which can in turn be assembled into constrained parallel robots. We demonstrate the formulation and solution of the dual quaternion design equations for the spatial RPRP chain.
[DOI: 10.1115/1.1737378]

1 Introduction

This paper presents a dual quaternion synthesis methodology for the design of robotic systems constructed from one or more serial chains, each of which imposes a constraint on the end-effector. These so-called ''constrained robotic systems'' provide structural support in certain directions while allowing freedom of movement in others.

Our design methodology parallels the well-known linkage synthesis techniques of planar and spherical kinematics. The kinematics equations of the chain are evaluated on a finite set of task positions, in order to define a set of design equations. These equations have both structural parameters and joint parameters as unknowns and can be solved for both. We find that an efficient procedure exists for eliminating the joint variables in the class of serial chains with constrained orientation. For the remainder of the chains, we outline a strategy for this elimination that becomes increasingly more complicated for chains with increasing numbers of structural parameters. Further work is needed to determine the maximum number of solutions to the design equations for a given chain, and to provide an efficient process for finding all of these solutions. The technique is demonstrated for the RPRP serial chain using both the complete equations with structural and joint parameters, and the equations obtained after the elimination of joint variables.

In what follows, we provide a literature review of robot synthesis theory, and then formulate the general dual quaternion design equations. It is possible to count the number of structural and joint parameters in order to determine the number of positions needed to completely define the serial chain. We then explore the algebraic structure of the dual quaternion design equations and conclude by solving the equations for the RPRP serial chain.

2 Literature Review

The finite-position synthesis theory seeks to dimension a serial kinematic chain that reaches a specified set of positions. This problem was first stated and solved by Schoenflies [1] and Burmester [2], and generalized to spatial chains by Roth [3]. See Hartenberg and Denavit [4] and Sandor and Erdman [5], for applications of this theory to planar chains, and Suh and Radcliffe [6], and McCarthy [7] for application to spherical and spatial chains. Several approaches have been developed to extend this design theory to spatial kinematic chains, that may be described as based on geometric constraints, the screw triangle, loop closure equations, and robot kinematics equations.

The *geometric constraint* method uses the geometric properties of two-jointed serial chains to formulate equations that must be satisfied at each of a discrete set of positions in the workspace, (Suh and Radcliffe [6], Hunt [8]). This yields algebraic equations that are solved to determine the dimensions of the chain. Examples of this are the synthesis of spatial RR chains (Suh [9]), CC chains (McCarthy [10], Huang and Chang [11], Kihonge et al. [12]), and SS chains (Innocenti [13], Liao and McCarthy [14]). This approach is limited to dyads and three-jointed chains ending in S joints, such as the RPS and PPS chains as well as the CS chain, see Chen and Roth [15], Nielsen and Roth [16], and also Kim and Tsai [17].

A generalization was introduced by Tsai and Roth [18] who used the geometry of the screw triangle associated with a sequence of transformations to formulate design equations for serial chains. Tsai's dissertation [19] provides a list of chains consisting of two and three joints and their associated design equations. This approach introduced intermediate joint parameters as necessary to describe the chains. In Tsai and Roth [20] they obtained an algebraic solution to the 10 design equations for the spatial RR chain, (also see Perez and McCarthy [21]).

Sandor [22] uses loop closure equations to create design equations for spatial linkages with any number of joints. This approach has been applied to spatial synthesis expressing the links as vectors and the rotations as matrices in Sandor and Bisshopp [23], Sandor, Weng, and Xu [24], and in Sandor, Xu, and Weng [25] they were used to state the design equations for spatial 3R and 4R spatial linkages. The loop equations characterize the translation of the mechanism, while they are parameterized by the joint variables; additional equations need to be added to account for orientations and extra parameters defining the links.

Mavroidis, Lee, and Alam [26] formulated and solved the design equations for the spatial RR chain using the homogeneous matrix form of the kinematics equations. They soon followed this with a solution for the RRR serial chain, and the PRR chain (Lee and Mavroidis 2002 [27,28,29]). Their approach introduces the Denavit-Hartenberg parameters, as well as the joint variables at each of the task positions, as the variables in the design equations. It can be systematically applied to a broad range of serial chains.

In this paper, we use Mavroidis' systematic approach; however, we use successive screw displacements, described by Gupta [30]

Contributed by the Mechanisms and Robotics Committee for publication in the JOURNAL OF MECHANICAL DESIGN. Manuscript received February 2003; revised October 2003. Associate Editor: C. Mavroidis.

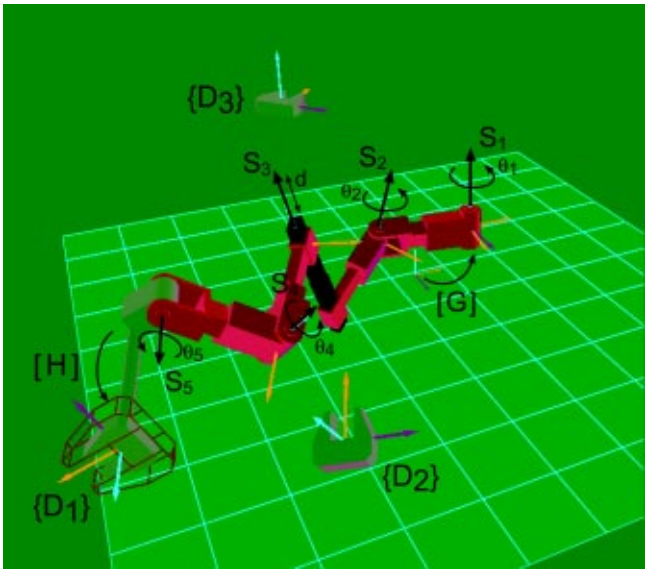

Fig. 1 A constrained serial robot and three specified task positions

and Tsai [31], formulated using dual quaternion algebra. Yang and Freudenstein [32] introduced dual quaternions to kinematics in order to define for three dimensional space a geometric algebra that parallels the convenience of complex numbers in the plane. These hypercomplex numbers form an eight dimensional Clifford algebra that can be used to define spatial displacements (McCarthy [33], Shoham and Jen [34], and Angeles [35]). Clifford algebras have been used in robot analysis, see for instance Ravani and Ge [36], and for the synthesis of planar linkages using planar quaternions, see Larochelle [37].

In our approach, the design equations contain the axes of the robot in a reference configuration, as in [22], parameterized by the joint variables. We use the Plücker coordinates of the joint axes as design parameters and obtain eight design equations for each task position, see [38]. Like in the previous work of Sandor [22], Tsai and Roth [18] and Lee and Mavroidis [28,29], the joint variables appear in our design equations, and we devise a procedure to eliminate them.

3 Kinematics Equations of a Serial Robot

The kinematics equations of the robot equate the 4×4 homogeneous transformation $[D]$ between the end-effector and the base frame to the sequence of local coordinate transformations along the m joint axes of the chain (Craig [39]),

$$[D]=[G][Z(\theta_1,d_1)][X(\alpha_{12},a_{12})]\times[Z(\theta_2,d_2)]\ldots[X(\alpha_{m-1,m},a_{m-1,m})][Z(\theta_m,d_m)][H]. \quad (1)$$

The parameters (θ,d) define the movement at each joint and (α,a) are the twist and length of each link, collectively known as the Denavit-Hartenberg parameters. The transformation $[G]$ defines the position of the base of the chain relative to the fixed frame, and $[H]$ locates the tool relative to the last link frame, see Fig. 1. Notice that for constrained serial chains $m\leqslant5$.

3.1 Successive Screw Displacements. These kinematics equations can be transformed into successive screw displacements by choosing a reference position $[D_0]$. Let $[D_i]$ be the homogeneous matrix describing the transformation from the fixed frame to a moving frame M_i. We can compute the relative transformation $[D_{0i}]=[D_i][D_0]^{-1}$, which expresses the displacement of the moving frame from the reference position, M_0, to the ith position, M_i, measured in the fixed frame,

$$[D_{0i}]=[D_i][D_0]^{-1},$$
$$=([G][Z(\theta_1^i,d_1^i)]\ldots[Z(\theta_m^i,d_m^i)][H])([G]\times[Z(\theta_1^0,d_1^0)]\ldots[Z(\theta_m^0,d_m^0)][H])^{-1}. \quad (2)$$

In order to simplify this equation we introduce the partial transformations $[M_j]$ up to but not including the jth joint transformation for the reference configuration, so we have

$$[M_1]=[G],$$
$$[M_2]=[G][Z(\theta_1^0,d_1^0)][X(\alpha_{12},a_{12})],$$
$$\ldots$$
$$[M_j]=[G][Z(\theta_1^0,d_1^0)][X(\alpha_{12},a_{12})]\times[Z(\theta_2^0,d_2^0)]\ldots[X(\alpha_{j-1,j}a_{j-1,j})]. \quad (3)$$

Equation (2) can now be rewritten in the form

$$[D_{0i}]=[T(\Delta\theta_1^i,\mathsf{S}_1)][T(\Delta\theta_2^i,\mathsf{S}_2)]\ldots[T(\Delta\theta_m^i,\mathsf{S}_m)], \quad (4)$$

where

$$[T(\Delta\theta_1^i,\mathsf{S}_1)]=[M_1][Z(\theta_1^i,d_1^i)][Z(\theta_1^0,d_1^0)]^{-1}[M_1]^{-1},$$
$$[T(\Delta\theta_2^i,\mathsf{S}_2)]=[M_2][Z(\theta_2^i,d_2^i)][Z(\theta_2^0,d_2^0)]^{-1}[M_2]^{-1},$$
$$\ldots$$
$$[T(\Delta\theta_j^i,\mathsf{S}_j)]=[M_j][Z(\theta_j^i,d_j^i)][Z(\theta_j^0,d_j^0)]^{-1}[M_j]^{-1}, \quad (5)$$

where $\Delta\theta_j^i=\theta_j^i-\theta_j^0$ or $\Delta\theta_j^i=d_j^i-d_j^0$ depending on whether the joint is revolute or prismatic, respectively.

The displacements $[T(\Delta\theta_i,\mathsf{S}_i)]$ define the rotations about and translations along the joint axes S_i measured in the fixed frame relative to the reference configuration $[D_0]$. Notice that by expressing kinematics equations in this way, the base transformation $[G]$ is absorbed into the coordinates of the first joint axis and the tool transformation $[H]$ cancels.

3.2 Dual Quaternion Kinematics Equations. The kinematics equations of the serial chain can be defined using elements of the Clifford algebra, known as *dual quaternions*, instead of 4×4 homogeneous transforms. The advantage is primarily a compact representation of the rotation matrix, and also a useful structure that assists the elimination of the joint variables. A spatial displacement consisting of a rotation by θ and slide by d around and along a screw axis S is written as the dual quaternion

$$\hat{S}(\hat{\theta})=\sin\left(\frac{\hat{\theta}}{2}\right)\mathsf{S}+\cos\left(\frac{\hat{\theta}}{2}\right), \quad (6)$$

where $\hat{\theta}=\theta+\epsilon d$ and $\mathsf{S}=\mathbf{S}+\epsilon\mathbf{p}\times\mathbf{S}$ is the dual vector formed from the Plücker coordinates of the screw axis. Recall that ϵ is the dual unit with the property $\epsilon^2=0$, (Bottema and Roth [40], McCarthy [33]), and that the sine and cosine of a dual angle are defined by

$$\cos\frac{\hat{\theta}}{2}=\cos\frac{\theta}{2}-\epsilon\frac{d}{2}\sin\frac{\theta}{2},\ \text{and}$$
$$\sin\frac{\hat{\theta}}{2}=\sin\frac{\theta}{2}+\epsilon\frac{d}{2}\cos\frac{\theta}{2}. \quad (7)$$

Notice that the dual quaternion in Eq. (6) encodes the same information as the 4×4 screw displacement matrix $[T(\Delta\theta,\mathsf{S})]$. Furthermore, the algebra of dual quaternions provides a multiplication operation that parallels the matrix multiplication of screw displacement matrices. Thus, we can define the dual quaternion

kinematics equations for the serial chain by simply replacing the 4×4 matrices in Eq. (4) by their dual quaternion equivalents to obtain

$$\hat{D}^i=\hat{S}_1(\Delta\hat{\theta}_1^i)\hat{S}_2(\Delta\hat{\theta}_2^i)\ldots\hat{S}_m(\Delta\hat{\theta}_m^i). \tag{8}$$

The Plücker coordinates of the screw axes S_i, $i=1,\ldots,m$, are defined in the base frame F and form convenient design parameters.

4 Design Equations

In kinematic synthesis the focus is on the design of a serial chain that can reach a prescribed set of task positions. These positions provide a discrete approximation to the workspace of the chain. Let the n positions be defined by the 4×4 transforms $[P_i]$, $i=1,\ldots,n$. Construct the $n-1$ relative transformation matrices $[P_{1i}]=[P_i][P_1]^{-1}$ and their associated dual quaternions $\hat{P}_{1i}$, $i=2,\ldots,n$. Equating the task dual quaternions $\hat{P}_{1i}$ to the kinematics equations (8) yields the design equations

$$\mathcal{Q}_i:\quad \hat{S}_1(\Delta\hat{\theta}_1^i)\hat{S}_2(\Delta\hat{\theta}_2^i)\ldots\hat{S}_m(\Delta\hat{\theta}_m^i)-\hat{P}_{1i}=0,\quad i=2,\ldots,n. \tag{9}$$

For the following calculations, we assume that each axis S_i defines either a revolute joint or a prismatic joint, but not both. This means the dual angle $\Delta\hat{\theta}_i=\Delta\theta_i+\epsilon\Delta d_i$ has only one variable, either $\Delta\theta_i$ or Δd_i. Other types of joints are created by adding constraints to the joint axes; for instance, a cylindrical joint (C) can be created as a revolute and a prismatic joint plus two constraints making the directions of both joint axes parallel.

Given a robot topology, the workspace of the robot admits a maximum number of arbitrary positions, which in turn define the dimensions of the workspace. When we define a task with the maximum number of positions for the robot topology, we obtain a finite number of robots which are solutions of the design equations. In what follows we explain how to calculate the maximum number of task positions for a given robot topology, based on counting the parameters of the design equations.

We distinguish between axes S_i that define revolute joints from those that define prismatic joints. The axis of a revolute joint is defined by four independent parameters in the associated Plücker coordinate vector. Coordinate-wise, the expression of a revolute joint consists on six elements, three for the direction and three for the moment, plus two constraints, which make the direction a unit vector and the moment perpendicular to the direction. In contrast, a prismatic joint depends only on two parameters that define the direction of the slide of the joint, that is, three coordinates defining a direction plus the unit vector constraint.

Let r and t be the number of revolute and prismatic joints in the chain, where $m=r+t$, then the number of structural parameters is $K=4r+2t$. Given n task positions, we also have $(n-1)r$ joint angles and $(n-1)t$ joint slides that must be determined. Thus, the total number of design parameters in an n-position task is $N=4r+2t+(n-1)r+(n-1)t$.

Only six of the eight components of a dual quaternion are independent, therefore only $6(n-1)$ of the design equations in (9) are independent. To these, we can add any equation c defining a constraint between the axes. We can equate the number of equations $E=6(n-1)+c$ and the number of unknowns N to obtain

$$n_{\max}=\frac{3r+t+6-c}{6-r-t},\quad r+t\leqslant5, \tag{10}$$

which defines the maximum number of task positions $n_{\max}$ needed to solve for the design variables in a constrained serial chain. Notice that $n_{\max}$ achieves a maximum of 21 task positions for the 5R chain. However, due to the semi-direct product structure of the group of rigid displacements, this formula is not always directly applicable and some cases must be distinguished.

Table 1 The orientation-limited constrained serial chains

Robot	DOF	r	t	K	n_R	$n_{\max}$	e
RP	2	1	1	6	2	$2\frac{1}{2}$	1
RPP	3	1	2	6	2	3	3
PRP	3	1	2	8	2	$3\frac{2}{3}$	5
RRPP	4	2	2	10	5	6	2
RPRP	4	2	2	12	5	7	4

4.1 Orientation Design Equations. The design equations can be separated into three that define the orientation of the end-effector and three that define its translation. The $3(n-1)$ orientation design equations include the $2r$ unknowns that define the directions of the revolute joints and $(n-1)r$ associated joint rotation angles. These equations can be solved for a maximum number of task orientations given by

$$n_R=\frac{3+r-c}{3-r},\quad r\leqslant2. \tag{11}$$

This equation is meaningful only for $r=1$ and $r=2$, which have the associated values of $n_R=2$ and $n_R=5$. For constrained serial chains in which $n_R<n_{\max}$, we can solve the orientation equations independent of the translation equations. We call serial chains that have this property ''orientation limited chains.'' Table 1 lists the classes of serial chains that are orientation limited—the ordering of the R and P joints is not relevant, except for the cases specified in the table, see [41] for more details.

An orientation-limited chain can actually be designed to reach more than n_R task positions. The key is to select excess positions that have orientations that lie in the workspace of the spherical chain obtained using the orientation design equations. This can be done by selecting the direction of the screw axis and the rotation angle belonging to the workspace of orientations, while the location of the screw axis and the translation along it can be arbitrarily chosen. Assuming that the orientations are given and that both the directions of the revolute joints and the angles to reach the task orientations are known, we can count, in a similar fashion, the number of translations that the chain can be defined for,

$$n_T=\frac{2r+t+3-c}{3-t},\quad t\leqslant2. \tag{12}$$

If $n_R<n_{\max}$, we can solve the chain for n_R complete task positions plus $e=n_T-n_R$ additional task positions with arbitrary translational terms and rotational terms within the workspace of the chain. The number of additional task positions e is listed in Table 1. See [41] for further discussion on the counting formulas.

Constrained serial chains that have three or more revolute joints are clearly not orientation-limited, in which case the number of task positions is defined by the parameter $n_{\max}$ given in (10). It is interesting to note that the spatial RR and the various RRP chains are also not orientation-limited. Table 2 lists the number of task positions $n_{\max}$ available for the design of these chains.

4.2 Chains With Cylindric Joints. The combination of a revolute joint and prismatic joint in series such that their axes are parallel is said to form a cylindric joint, denoted C. We view this combination as imposing the $c=2$ constraints on the six parameters of the RP combination, in particular that the direction of the P-joint be the same as that of the R-joint. Tables 3 and 4 list the classes of constrained serial chains that have cylindric joints and the number of task positions that they can reach.

5 Parameterized Design Equations

To solve for a given robot structure, we compute the maximum number of goal positions using n_R and $n_{\max}$, define extra constraints for the axes if needed, and apply Eq. (9) for the n goal dual quaternions. We obtain a set of $6(n-1)+c$ equations, where c is the number of structural constraints we add to the general

Table 2 Constrained serial chains that are not orientation-limited

Robot	DOF	r	t	K	$n_{\max}$
RR	2	2	0	8	3
RRP	3	2	1	10	$4\frac{1}{3}$
RRR	3	3	0	12	5
RRRP	4	3	1	14	8
RRRR	4	4	0	16	9
RRRPP	5	3	2	14	15
RRPRP	5	3	2	16	17
RRRRP	5	4	1	18	19
RRRRR	5	5	0	20	21

structure. As the set of equations we use the six independent components of the dual quaternion equality plus the Plücker constraints for each axis,

$$Q^i=\begin{Bmatrix} q_x+\epsilon q_{x0} \\ q_y+\epsilon q_{y0} \\ q_z+\epsilon q_{z0} \end{Bmatrix}^i = \begin{Bmatrix} p_x+\epsilon p_{x0} \\ p_y+\epsilon p_{y0} \\ p_z+\epsilon p_{z0} \end{Bmatrix}^i, \quad i=2,\ldots n,$$

$$\mathbf{s}_j\cdot\mathbf{s}_j=1, \quad \mathbf{s}_j\cdot\mathbf{s}_j^0=0, \quad j=1,\ldots r,$$

$$\mathbf{s}_k\cdot\mathbf{s}_k=1, \quad k=1,\ldots t, \tag{13}$$

and any extra geometric constraint we want to add.

We call Eq. (13) the *parameterized design equations*. In this set of equations, we solve for the structural parameters defining the joint axes at the reference position, but also for the values of each of the joint variables to reach each of the task positions. Notice that solving also for the joint variables increases the dimension of the problem by $(r+t)(n-1)$. For instance, for the PRRR robot, the number of total variables is 49, out of which 28 correspond to the values of the joint variables, and for the 5R robot the total number of variables is 130, out of which 100 correspond to joint variables. The number of solutions we have to track tends also to increase because of the multiple solutions for the inverse kinematics.

6 Inverse Kinematics Elimination

The parameterized design equations can be solved directly for both joint axes and joint variables by using some numerical method. However, we may want to eliminate the joint variables, if possible, to obtain a set of equations whose only variables are the coordinates of the joint axes. We call this process *inverse kinematics elimination*. This elimination reduces the dimension of the system by $(r+t)(n-1)$.

The elimination takes place at each goal dual quaternion and while eliminating the joint variables, it provides formulas for the inverse kinematics of the robot. The procedure used here is general and can be constructed systematically; however, there are different ways of choosing the number and order of the joint variables that we want to eliminate. For a further discussion on the elimination procedure see Perez [41].

Consider the design equations in (9). We transform the set of eight equations for a generic goal dual quaternion $\hat{P}$ to a linear system of quaternions,

$$\hat{Q}(\hat{\theta}_1,\ldots,\hat{\theta}_k)=[\hat{M}]\hat{V}(\hat{\theta}_1,\ldots,\hat{\theta}_l)=\hat{P}. \tag{14}$$

Table 3 The orientation-limited chains with cylindric joints

Robot	DOF	r	t	C	K	n_R	$n_{\max}$	e
PC	3	1	2	3	6	2	$2\frac{2}{3}$	2
RPC	4	2	2	3	10	5	$5\frac{1}{2}$	1
PRC	4	2	2	2	10	5	6	2

Table 4 Chains with cylindric joints that are not orientation-limited

Robot	DOF	r	t	C	K	$n_{\max}$
C	2	1	1	2	4	2
RC	3	2	1	2	8	$3\frac{2}{3}$
CC	4	2	2	4	8	5
RRC	4	3	1	2	12	7
RCC	5	3	2	4	12	13
RRPC	5	3	2	3	14	14
RPRC	5	3	2	2	14	15
RRRC	5	4	1	2	16	17

The vector $\hat{V}$ contains only joint variables and the matrix $[\hat{M}]$ contains the structural variables. Solving the linear system, we eliminate the joint variables contained in the vector,

$$\hat{V}(\hat{\theta}_1,\ldots,\hat{\theta}_l)=[\hat{M}]^{-1}\hat{P}. \tag{15}$$

The solution of the system provides the inverse kinematics, and the relations among the variables in $\hat{V}$ are used to define the reduced design equations. This general procedure will be developed in detail for the example below.

7 The Spatial RPRP Robot

In this section we examine the spatial RPRP robot and formulate its dual quaternion kinematics equations. We obtain its design equations and count how many positions we can specify. We solve the general RPRP using polynomial continuation, and then examine the special case of the RPC, in which the axes of the final RP joints are parallel, and obtain an algebraic solution.

7.1 The General RPRP Robot. The spatial RPRP robot is a four-degree-of-freedom robot. The fixed axis $\mathsf{G}=\mathbf{g}+\epsilon\mathbf{g}^0$ allows rotation of angle θ about it. This is followed by a translation d along an arbitrary direction $\mathbf{h}$, a rotation of angle ϕ about an arbitrary axis $\mathsf{W}=\mathbf{w}+\epsilon\mathbf{w}^0$, and a translation b along an arbitrary direction $\mathbf{u}$, see Fig. 2.

7.1.1 The Design Equations for the RPRP Robot. The dual quaternion kinematics equations are obtained by composing the dual quaternions that represent each joint axis,

$$\hat{Q}_{RPRP}(\theta,d,\phi,b)=\hat{G}(\theta,0)\hat{H}(0,d)\hat{W}(\phi,0)\hat{U}(0,b) \tag{16}$$

We use the formulas in Eq. (10) and Eq. (11) with $r=2$, $t=2$ to count the maximum number of goal dual transformations that we can specify. We obtain $n_{\max}=7$ and $n_R=5$, which means the RPRP

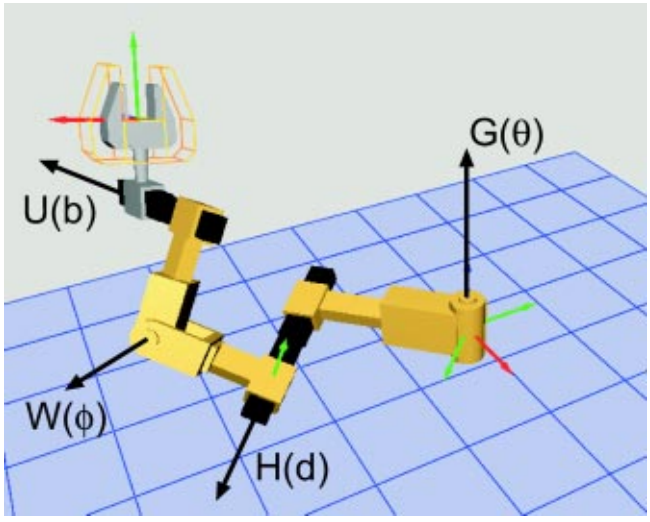

Fig. 2 The RPRP robot

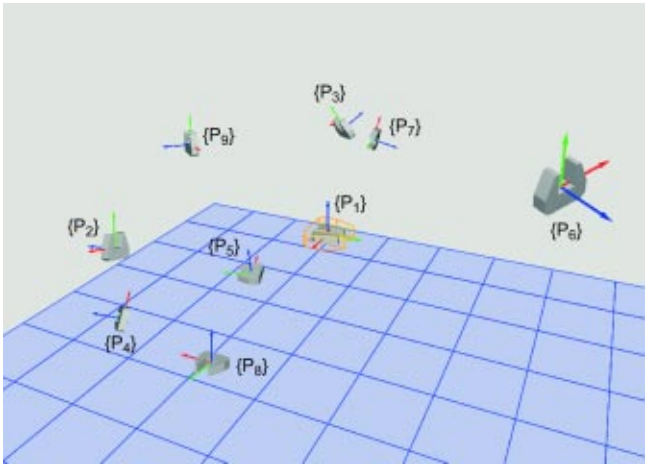

Fig. 3 The five complete plus four translational task positions

is orientation limited, Table 1. The maximum number of complete positions we can specify is five. In addition, we can specify four more positions with arbitrary translations, but with orientations that lie in the orientation workspace of the RPRP robot.

The design equations for the complete positions are obtained by equating the expressions in Eq. (16) to the goal dual quaternions,

$$\hat{Q}_{RPRP}(\theta^{1i},d^{1i},\phi^{1i},b^{1i})=\hat{P}^{1i},\quad i=2,3,4,5, \tag{17}$$

and the design equations for the partially specified positions by equating the dual components of Eq. (16), Q^0_{RPRP}, to the dual components of the four extra dual quaternions,

$$\hat{Q}^0_{RPRP}(\theta^{1i},d^{1i},\phi^{1i},b^{1i})=\hat{P}^{1i}_0,\quad i=6,7,8,9. \tag{18}$$

7.1.2 Solving the Design Equations for the RPRP Robot. We define five complete task dual quaternions randomly. They are labeled 1 to 5 in Table 6 and Fig. 3.

We can solve separately for the directions of the revolute joint axes **g** and **w** using the real part of each dual quaternion equality in Eq. (17). The quaternion for the spherical RR robot, $\hat{q}_{RR}=q_0+\mathbf{q}$, is expanded to

$$q_0=\cos\frac{\theta}{2}\cos\frac{\phi}{2}-\mathbf{g}\cdot\mathbf{w}\sin\frac{\theta}{2}\sin\frac{\phi}{2}$$

$$\mathbf{q}=\mathbf{g}\sin\frac{\theta}{2}\cos\frac{\phi}{2}+\mathbf{w}\cos\frac{\theta}{2}\sin\frac{\phi}{2}+\mathbf{g}\times\mathbf{w}\sin\frac{\theta}{2}\sin\frac{\phi}{2}. \tag{19}$$

We can either solve the parameterized equations for the real part only shown in Eq. (19), or use the inverse kinematics elimination. The elimination process, which is the same for every robot with two revolute joints, is the one presented below for the RPC robot, and yields six complex solutions [10]. For our task positions only two solutions are real, see Table 5.

We can now define the workspace of orientations of the robot for each of the real solutions. For this example we used solution 4 of Table 5. We can pick any orientation belonging to the workspace to construct the four additional dual quaternions with arbitrary translations. These are shown in Table 6 as the Plücker coordinates of the screw axis, the rotation about and the translation along the axis. The complete set of task positions appears in Fig. 3.

The design equations contain the dual parts only, that is,

$$Q^0=\begin{Bmatrix}q_{x0}\\q_{y0}\\q_{z0}\end{Bmatrix}^{1i}=\begin{Bmatrix}p_{x0}\\p_{y0}\\p_{z0}\end{Bmatrix}^{1i},\quad i=2,\ldots 9,$$

$$\mathbf{h}\cdot\mathbf{h}=1,\quad \mathbf{u}\cdot\mathbf{u}=1,$$

Table 5 Solutions for the orientations of the revolute joints

Joint Axis	*Direction*
g	$(-1.06+0.09i,-0.40+0.31i,0.38+0.58i)$
w	$(-0.29-0.08i,0.76+0.96i,1.27-0.59i)$
g	$(-1.06-0.09i,-0.40-0.31i,0.38-0.58i)$
w	$(-0.29+0.08i,0.76-0.96i,1.27+0.59i)$
g	(−0.48, −0.78, 0.39)
w	(0.33, −0.23, 0.91)
g	(0.04, 0.05, 0.99)
w	(0.70, 0.48, 0.53)
g	$(0.47-0.40i,-1.27-0.18i,0.06-0.80i)$
w	$(1.06-0.05i,0.15-0.30i,0.27+0.36i)$
g	$(0.47+0.40i,-1.27+0.18i,0.06+0.80i)$
w	$(1.06+0.049i,0.15+0.30i,0.27-0.36i)$

$$\mathbf{g}\cdot\mathbf{g}^0=0,\quad \mathbf{w}\cdot\mathbf{w}^0=0. \tag{20}$$

We create the linear system for the prismatic joint variables d and b,

$$[M_{db}]\begin{Bmatrix}d\\b\\1\end{Bmatrix}=\begin{Bmatrix}0\\0\\0\end{Bmatrix} \tag{21}$$

and solve linearly for them. The condition for a solution to exist is $\det[M_{db}]=0$. This condition yields one design equation per position, which is free of joint variables. Using the Plücker conditions to eliminate two of the variables, the final set of design equations has the structure

$$\mathcal{M}^i:\ h_x(A_{11}u_x+A_{12}u_y+A_{13}u_z)+h_y(A_{21}u_x+A_{22}u_y+A_{23}u_z)+h_z(A_{31}u_x+A_{32}u_y+A_{33}u_z)=0,\quad i=1,\ldots,8, \tag{22}$$

where the A_{ij} are linear functions of $\mathbf{g}_0$ and $\mathbf{w}_0$, $A_{ij}=C_1+C_2g_{x0}+C_3g_{y0}+C_4g_{z0}+C_5w_{x0}+C_6w_{y0}+C_7w_{z0}$. The equations are multi-linear in the components of **h**, **u** and $\{\mathbf{g}_0,\mathbf{w}_0\}$. We use the Plücker conditions to eliminate four of the variables. Due to the structure of the equations, a simple elimination of the components of $\mathbf{w}_0$ allows us to transform this set of equations in the final set of six cubic equations in six variables.

This set of six multi-linear equations in **h**, **u** and $\mathbf{g}^0$ has a total degree of 729. We obtain a sharper bound for the number of roots by computing the linear product decomposition (LPD) Bezout number, which is 90 (Verschelde [42]). We solve these equations using the polynomial homotopy continuation software PHC developed by Verschelde [42].

A random linear product start system with 240 start solutions was used, and it took the program 7.5 minutes on a PowerPC G4 at 733 MHz to find all solutions associated with each of the two real solutions of (19). In the first case, PHC yields 68 solutions of which 21 are regular and, of those, 7 are real roots. For the second case, PHC yields 21 regular solutions with 5 real roots. An ex-

Table 6 The five complete plus four translational goal positions

Position	*Axis*	*Rot.* (rad)	*Trans.*
1	(1.0, 0.0, 0.0; 0.0, 0.0, 0.0)	0	0
2	(0.98, −0.14, 0.16; −0.51, −1.81, 1.51)	1.75	2.21
3	(0.28, −0.46, −0.84; −0.01, −2.18, 1.20)	2.34	−1.20
4	(0.44, −0.31, 0.84; −2.61, −1.41, 0.86)	2.82	−0.68
5	(−0.08, −0.01, −0.99; 1.09, −0.43, −0.09)	2.83	1.85
6	(0.35, 0.69, 0.63; 0.44, −0.44, 0.23)	2.92	5.72
7	(−0.61, −0.64, −0.46; −0.51, −0.98, 2.04)	2.16	4.17
8	(−0.09, 0.08, 0.99; −1.62, −0.30, −0.12)	4.71	−2.48
9	(0.82, 0.37, 0.44; −0.92, −0.75, 2.33)	1.74	−2.75

Table 7 An RPRP robot that reaches 5 complete positions plus 4 translations

Joint Axis	*Direction*	*Moment*
G	(0.04, 0.05, 0.99)	(−2.12, −3.55, 0.25)
H	(−0.46, 0.63, 0.63)	(−2.22, −3.22, 1.62)
W	(0.70, 0.48, 0.53)	(−0.35, −2.42, 2.62)
U	(−0.82, −0.12, −0.56)	(0.33, 3.06, −1.17)

ample solution is listed in Table 7 and presented in Fig. 4 and 5. The RPRP robot was displayed using the software SYNTHETICA, [43] and [44].

7.2 Special Case: The RPC Robot. The design equations of the RPRP robot are specialized to those of the RPC robot by imposing the following set of constraints:

$$\mathbf{g}\cdot\mathbf{h}=0, \quad \mathbf{w}\cdot\mathbf{h}=0, \quad \mathbf{w}\times\mathbf{u}=\vec{0}. \tag{23}$$

This defines an RPC robot that has its P-joint perpendicular to the axes of the R and C joints.

The RPC robot is a four-degree-of-freedom robot. The fixed axis $\mathsf{G}=\mathbf{g}+\epsilon\mathbf{g}^0$ allows rotation of angle θ about it. This is followed in the chain by a translation d along a direction $\mathbf{h}$ and finally a rotation of angle ϕ and a translation b along an axis $\mathsf{W}=\mathbf{w}+\epsilon\mathbf{w}^0$, see Fig. 6.

7.2.1 Kinematics Equations for the RPC Robot. The dual quaternion kinematics equations are obtained by composing the dual quaternions that represent each joint axis,

$$\hat{Q}_{RPC}(\theta,d,\phi,b)=\hat{G}(\theta,0)\hat{H}(0,d)\hat{W}(\phi,b). \tag{24}$$

We expand Eq. (24), $\hat{Q}_{RPC}=\hat{Q}_0+\mathsf{Q}$, to obtain

$$\begin{aligned}\hat{Q}_0=&c\frac{\theta}{2}c\frac{\phi}{2}-\mathbf{g}\cdot\mathbf{w}s\frac{\theta}{2}s\frac{\phi}{2}\\&+\epsilon\left(-\left(\frac{d}{2}\mathbf{g}\cdot\mathbf{h}+\frac{b}{2}\mathbf{g}\cdot\mathbf{w}\right)s\frac{\theta}{2}c\frac{\phi}{2}-\left(\frac{b}{2}+\frac{d}{2}\mathbf{h}\cdot\mathbf{w}\right)c\frac{\theta}{2}s\frac{\phi}{2}\right.\\&\left.+\left(\frac{d}{2}(\mathbf{g}\times\mathbf{w})\cdot\mathbf{h}-(\mathbf{g}_0\cdot\mathbf{w}+\mathbf{g}\cdot\mathbf{w}_0)\right)s\frac{\theta}{2}s\frac{\phi}{2}\right),\end{aligned} \tag{25}$$

$$\begin{aligned}\mathsf{Q}=&\mathbf{g}s\frac{\theta}{2}c\frac{\phi}{2}+\mathbf{w}c\frac{\theta}{2}s\frac{\phi}{2}+\mathbf{g}\times\mathbf{w}s\frac{\theta}{2}s\frac{\phi}{2}\\&+\epsilon\left(\left(\mathbf{g}_0+\frac{b}{2}\mathbf{g}\times\mathbf{w}+\frac{d}{2}\mathbf{g}\times\mathbf{h}\right)s\frac{\theta}{2}c\frac{\phi}{2}\right.\\&+\left(\mathbf{w}_0+\frac{d}{2}\mathbf{h}\times\mathbf{w}\right)c\frac{\theta}{2}s\frac{\phi}{2}+\left(\frac{b}{2}\mathbf{w}+\frac{d}{2}\mathbf{h}\right)c\frac{\theta}{2}c\frac{\phi}{2}\\&\left.+\left(\mathbf{g}_0\times\mathbf{w}+\mathbf{g}\times\mathbf{w}_0-\frac{b}{2}\mathbf{g}+\frac{d}{2}(\mathbf{g}\cdot\mathbf{w})\mathbf{h}\right)s\frac{\theta}{2}s\frac{\phi}{2}\right),\end{aligned} \tag{26}$$

where c and s stand for cosine and sine respectively.

7.2.2 The Design Equations for the RPC Robot. Using Eq. (10), we compute the number of complete positions, with $r=2$, $t=2$, but considering the constraints in Eq. (23). We obtain $n_{\max}=5$ complete spatial goal positions, same value that we obtain for n_R. In this case we can solve for five complete task positions.

For the direct solution of the parameterized equations, which is presented later, we just need to equate the expressions in Eq. (25) and Eq. (26) to the task dual quaternions,

$$\hat{Q}_{RPC}(\theta^{1i},d^{1i},\phi^{1i},b^{1i})=\hat{P}^{1i}, \quad i=2,3,4,5. \tag{27}$$

7.2.3 Inverse Kinematics Elimination for the RPC Robot We can write the design equations in Eq. (27) as the linear transformation

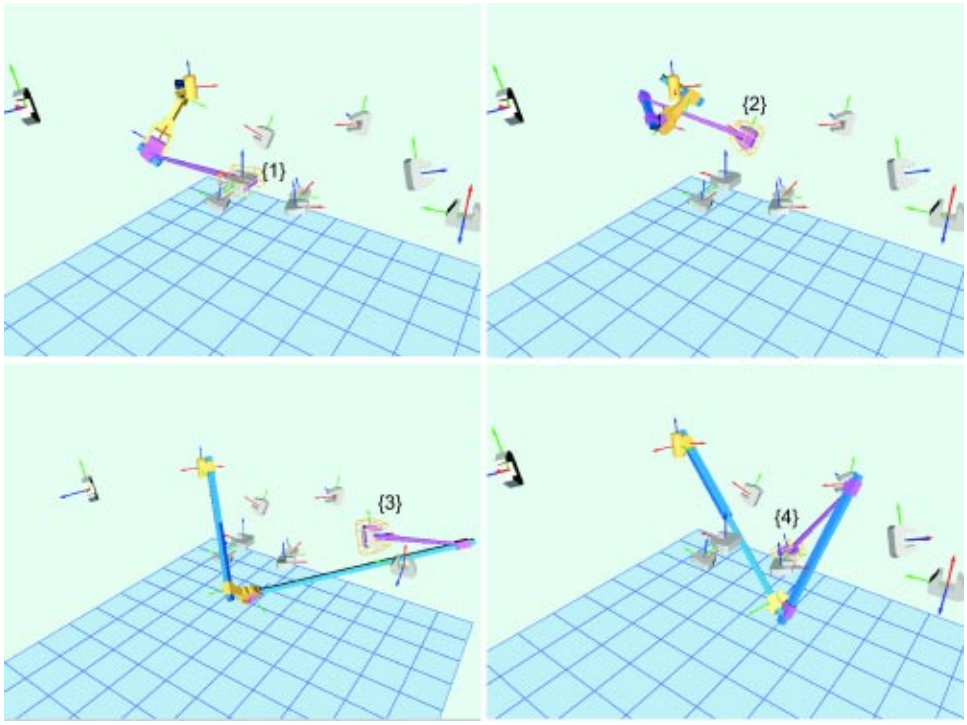

Fig. 4 The RPRP robot reaching the task positions 1, 2, 3 and 4

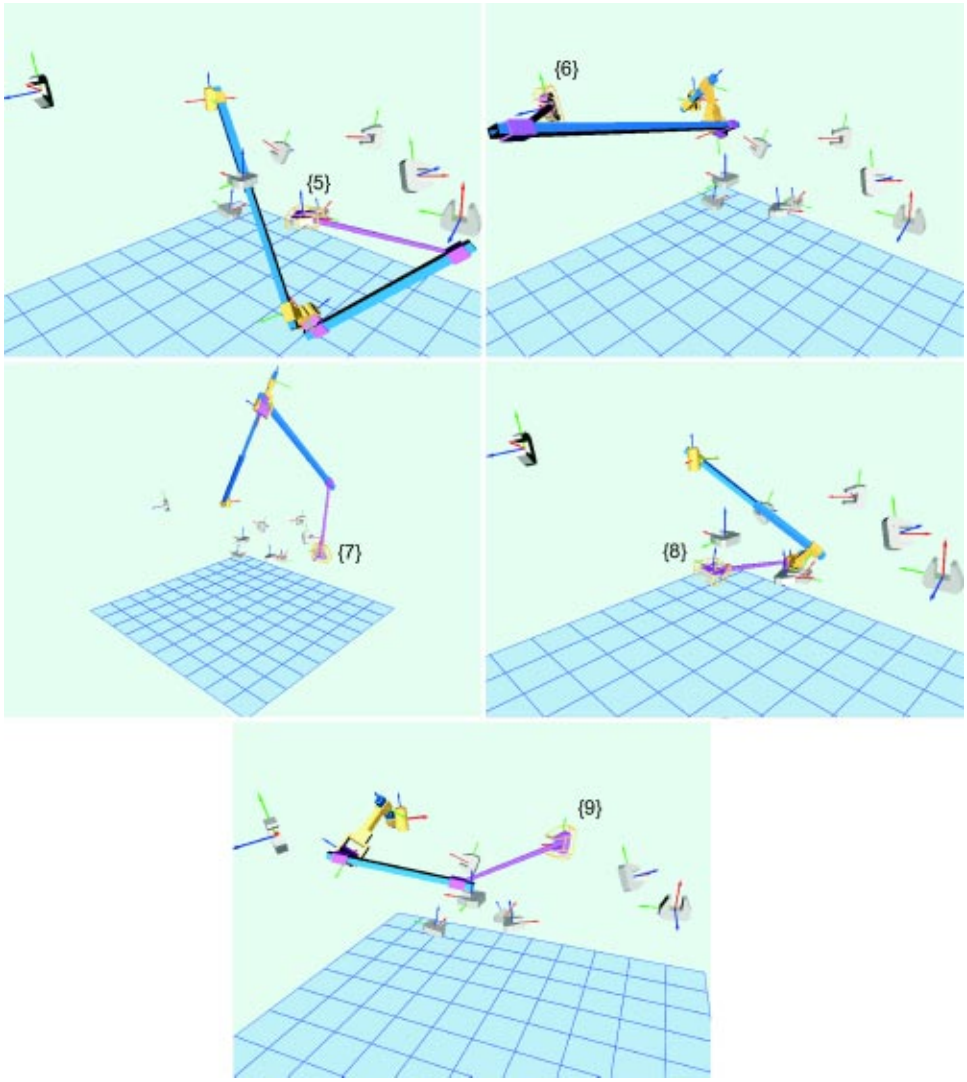

Fig. 5 The RPRP robot reaching the task positions 5, 6, 7, 8, and 9

$$\hat{Q}_{RPC}(\theta,d,\phi,b)=[\hat{M}]\hat{V}(\theta,\phi,d)=\hat{P}, \tag{28}$$

where $\hat{V}$ is

$$\hat{V}(\theta,\phi,d)=\begin{Bmatrix} \sin\frac{\theta}{2}\cos\frac{\phi}{2}+\epsilon\frac{d}{2}\cos\frac{\theta}{2}\sin\frac{\phi}{2} \\ \cos\frac{\theta}{2}\sin\frac{\phi}{2}+\epsilon\frac{d}{2}\sin\frac{\theta}{2}\cos\frac{\phi}{2} \\ \sin\frac{\theta}{2}\sin\frac{\phi}{2}+\epsilon\frac{d}{2}\cos\frac{\theta}{2}\cos\frac{\phi}{2} \\ \cos\frac{\theta}{2}\cos\frac{\phi}{2}+\epsilon\frac{d}{2}\sin\frac{\theta}{2}\sin\frac{\phi}{2} \end{Bmatrix}. \tag{29}$$

If we write the dual quaternions as 8-dimensional vectors, the matrix $[\hat{M}]$ of Eq. (28) has the form:

$$[\hat{M}]=\begin{bmatrix} A & \vdots & 0 \\ \cdots & & \cdots \\ B & \vdots & C \end{bmatrix} \tag{30}$$

where the submatrices are

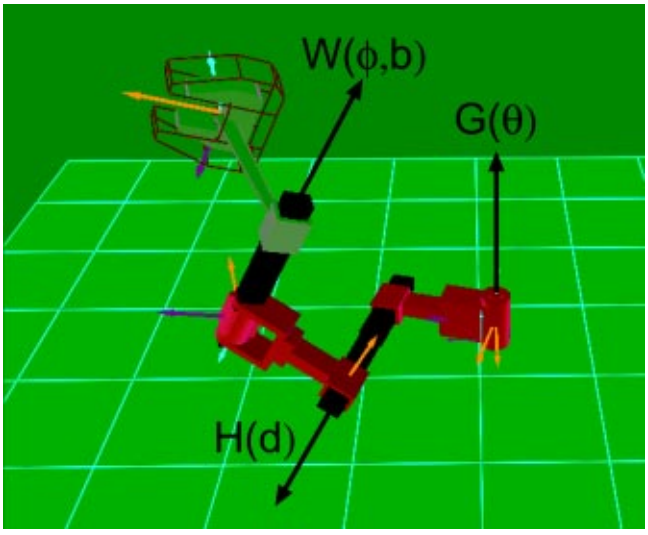

Fig. 6 The RPC robot

$$[A]=\begin{bmatrix}\mathbf{g} & \mathbf{w} & \mathbf{g}\times\mathbf{w} & 0\\ 0 & 0 & -\mathbf{g}\cdot\mathbf{w} & 1\end{bmatrix}, \tag{31}$$

$$[B]=\begin{bmatrix}\mathbf{g}^0+\dfrac{b}{2}\mathbf{g}\times\mathbf{w} & \mathbf{w}^0 & \mathbf{g}^0\times\mathbf{w}+\mathbf{g}\times\mathbf{w}^0-\dfrac{b}{2}\mathbf{g} & \dfrac{b}{2}\mathbf{w}\\ -\dfrac{b}{2}\mathbf{g}\cdot\mathbf{w} & -\dfrac{b}{2} & -(\mathbf{g}^0\cdot\mathbf{w}+\mathbf{g}\cdot\mathbf{w}^0) & 0\end{bmatrix} \tag{32}$$

and

$$[C]=\begin{bmatrix}\mathbf{h}\times\mathbf{w} & \mathbf{g}\times\mathbf{h} & \mathbf{h} & (\mathbf{g}\cdot\mathbf{w})\mathbf{h}\\ -\mathbf{h}\cdot\mathbf{w} & -\mathbf{g}\cdot\mathbf{h} & 0 & (\mathbf{g}\times\mathbf{w})\cdot\mathbf{h}\end{bmatrix}. \tag{33}$$

We solve for the components of the vector $\hat{V}$ by inverting the matrix $[\hat{M}]$,

$$\hat{V}(\theta,\phi,d)=\begin{bmatrix}A^{-1} & \vdots & 0\\ \cdots & & \cdots\\ -C^{-1}BA^{-1} & \vdots & C^{-1}\end{bmatrix}\hat{P} \tag{34}$$

The matrices are invertible for nondegenerated cases. The determinant of the matrix $[A]$ is equal to $(\mathbf{g}\times\mathbf{w})\cdot(\mathbf{g}\times\mathbf{w})$; it is nonzero when the joint axes are not parallel. Similarly, the determinant of matrix $[C]$ is $\mathbf{h}\cdot(\mathbf{g}\times\mathbf{w})$. The inverses of these submatrices are easily expressed as row vectors; their expressions as matrices of row vectors can be found in the Appendix.

We solve for the rotational components of $\hat{V}$,

$$\begin{Bmatrix}\sin\dfrac{\theta}{2}\cos\dfrac{\phi}{2}\\ \cos\dfrac{\theta}{2}\sin\dfrac{\phi}{2}\\ \sin\dfrac{\theta}{2}\sin\dfrac{\phi}{2}\\ \cos\dfrac{\theta}{2}\cos\dfrac{\phi}{2}\end{Bmatrix}=[A]^{-1}\hat{P}_R, \tag{35}$$

and for the translational components,

$$\begin{Bmatrix}\dfrac{d}{2}\cos\dfrac{\theta}{2}\sin\dfrac{\phi}{2}\\ \dfrac{d}{2}\sin\dfrac{\theta}{2}\cos\dfrac{\phi}{2}\\ \dfrac{d}{2}\cos\dfrac{\theta}{2}\cos\dfrac{\phi}{2}\\ \dfrac{d}{2}\sin\dfrac{\theta}{2}\sin\dfrac{\phi}{2}\end{Bmatrix}=-([C]^{-1}[B][A]^{-1})\hat{P}_R+[C]^{-1}\hat{P}_0, \tag{36}$$

where $\hat{P}_R=\mathbf{p}+p_w$, $\hat{P}_0=\mathbf{p}^0+p_{w0}$.

Notice that the solution in Eq. (35), presented in the Appendix, corresponds to any robot with two revolute joints, and together Eq. (35) and Eq. (36) give the inverse kinematics for the joint variables θ, ϕ, and d. The solutions of Eq. (36) contain the joint variable b that we eliminate below.

To create the reduced design equations we use the relations among the variables we solved for in Eq. (35) and Eq. (36). For the rotational components, the relation $\mathcal{R}$ is

$$\mathcal{R}:\ \frac{\sin\dfrac{\theta}{2}\sin\dfrac{\phi}{2}}{\cos\dfrac{\theta}{2}\sin\dfrac{\phi}{2}}=\frac{\sin\dfrac{\theta}{2}\cos\dfrac{\phi}{2}}{\cos\dfrac{\theta}{2}\cos\dfrac{\phi}{2}}. \tag{37}$$

Substitute the values obtained solving Eq. (35) (see Appendix) and collect terms to obtain the first reduced design equation $\mathcal{R}$,

$$(p_w\mathbf{g}\cdot\mathbf{p}\times\mathbf{w}+\mathbf{g}\cdot(\mathbf{p}\times(\mathbf{p}\times\mathbf{w})))(\mathbf{g}\times\mathbf{w}\cdot\mathbf{g}\times\mathbf{w})^2/(\mathbf{g}\times\mathbf{w}\cdot\mathbf{g}\times\mathbf{w})=0 \tag{38}$$

If we require that $\mathbf{g}\times\mathbf{w}\neq 0$, which restricts the pair of revolute joints from generating a pure planar movement, then we obtain

$$\mathcal{R}_1:\quad p_w\mathbf{g}\cdot\mathbf{p}\times\mathbf{w}+\mathbf{g}\cdot(\mathbf{p}\times(\mathbf{p}\times\mathbf{w}))=0. \tag{39}$$

It is interesting to notice that this equation corresponds to both the matrix equation and the equivalent screw triangle formulation in the following way,

$$\mathcal{R}_1=\mathbf{g}\cdot([A_{Euler}-I]\mathbf{w})=\tan\frac{\psi}{2}-\frac{\mathbf{g}\cdot(\mathbf{p}_u\times\mathbf{w})}{(\mathbf{p}_u\times\mathbf{g})\cdot(\mathbf{p}_u\times\mathbf{w})}, \tag{40}$$

where A_{Euler} is the expression of the rotation matrix obtained using the Euler parameters, and $\mathbf{p}_u=\mathbf{p}/|\mathbf{p}|$ with $\sin\psi/2=|\mathbf{p}|$ and $\cos\psi/2=p_w$.

Same procedure can be applied to the variables we solve for in Eq. (36). Being careful to choose the relations that make the equations well-conditioned, we can define the two independent relations

$$\mathcal{L}_1:\ \frac{\dfrac{d}{2}\cos\dfrac{\theta}{2}\cos\dfrac{\phi}{2}}{\cos\dfrac{\theta}{2}\cos\dfrac{\phi}{2}}=\frac{\dfrac{d}{2}\sin\dfrac{\theta}{2}\sin\dfrac{\phi}{2}}{\sin\dfrac{\theta}{2}\sin\dfrac{\phi}{2}},$$

$$\mathcal{L}_2:\ \frac{\dfrac{d}{2}\cos\dfrac{\theta}{2}\sin\dfrac{\phi}{2}}{\cos\dfrac{\theta}{2}\sin\dfrac{\phi}{2}}=\frac{\dfrac{d}{2}\sin\dfrac{\theta}{2}\cos\dfrac{\phi}{2}}{\sin\dfrac{\theta}{2}\cos\dfrac{\phi}{2}}. \tag{41}$$

With the solution of Eq. (36), whose expression can be found in the Appendix, we obtain two linear equations in b. If we denote them $\mathcal{L}_1: A_1b/2+B_1=0$, $\mathcal{L}_2: A_2b/2+B_2=0$, we create the second reduced design equation by equating both solutions for b,

$$\mathcal{R}_2:\quad \frac{B_1}{A_1}=\frac{B_2}{A_2}. \tag{42}$$

These two reduced design equations, plus the set of Plücker and extra constraints, form the final set of 15 reduced equations in 15 parameters,

$$\begin{gathered}\{\mathcal{R}_1,\mathcal{R}_2\}^i,\quad i=1,\ldots 4,\\ \mathbf{g}\cdot\mathbf{g}=1,\quad \mathbf{g}\cdot\mathbf{g}_0=0,\\ \mathbf{w}\cdot\mathbf{w}=1,\quad \mathbf{w}\cdot\mathbf{w}_0=0,\\ \mathbf{h}\cdot\mathbf{h}=1,\quad \mathbf{h}\cdot\mathbf{g}=0,\quad \mathbf{h}\cdot\mathbf{w}=0.\end{gathered} \tag{43}$$

7.2.4 Solving the Design Equations for the RPC Robot. The reduced equations (43) can be solved algebraically. Notice that we can again solve for the revolute joint directions $\mathbf{g}$ and $\mathbf{w}$ separately in the revolute equations $\mathcal{R}_1$. Once we have those, the direction $\mathbf{h}$ is completely specified by the two constraints in Eq. (23). The translation equations $\mathcal{R}_2$ are linear in the moment components of the revolute joint axes, $\mathbf{g}^0$ and $\mathbf{w}^0$.

The algebraic solution for the direction $\mathbf{g}$ and $\mathbf{w}$ is obtained as for RR spherical chains, see McCarthy [10]. It consists of a two-step elimination procedure that yields a sixth degree polynomial. This polynomial yields an even number of real roots. As the translation equations are linear, the total number of solutions for the RPC robot is equal to the number of solutions for the orientations, that is, six complex solutions.

For our design example, the goal displacements shown on Table 8 and Fig. 7 have been randomly generated. The algebraic solution of the reduced design equations yields six solutions, out of

Table 8 The goal positions

Axis	*Rot.* (rad)	*Trans.*
(1.0, 0.0, 0.0; 0.0, 0.0, 0.0)	0	0
(0.33, −0.26, 0.91; 0.60, −1.02, −0.50)	2.28	0.32
(0.52, −0.56, 0.64; 1.10, 1.47, 0.37)	1.43	−0.27
(0.32, −0.84, 0.43; −0.70, 0.00, 0.52)	5.09	1.66
(−0.55, 0.07, −0.83; −1.31, −0.03, 0.86)	4.55	1.09

which two are real, see Table 9. The synthesis procedure was implemented in the design software SYNTHETICA [43], see Fig. 8.

8 Conclusions

This paper introduces a dual quaternion formulation for the kinematic synthesis of constrained serial chains. The kinematics equations of the chain are transformed to successive screw displacements, and then written in dual quaternion form. These dual quaternion kinematics equations are evaluated at a finite set of task positions to yield design equations for the chain.

A count of the number of design parameters and design equations yields the number of task positions needed to determine the dimensions of a given class of constrained serial chains. We find that chains with one or two revolute joints can be orientation-limited, in which case a strategy exists that allows the synthesis of these chains such that they reach an excess positions using the translation equations.

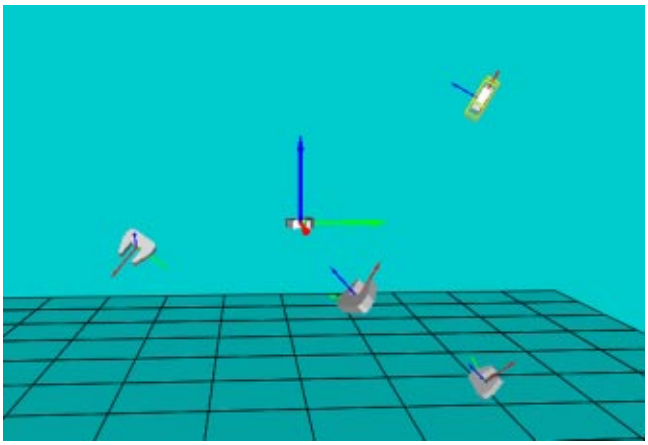

Fig. 7 The goal positions

We demonstrate this theory by formulating the design equations for the RPRP serial chain, which is orientation-limited, and solve these equations using polynomial continuation. We also formulate and solve the design equations for the RPC chain, which is a special case of the RPRP robot. The design equations for this chain can be solved algebraically. The results show that the dual quaternion design equations provide a convenient and useful tool for the synthesis of constrained serial chains.

Acknowledgments

The authors gratefully acknowledge the support of National Science Foundation award 0218285 and interactions with Haijun Su of the UCI Robotics and Automation Laboratory and Prof. Bruce Bennett of the UCI Department of Mathematics. Also acknowledged are the many valuable comments and recommendations by the reviewers.

Appendix

The inverses of the submatrices of Eq. (34) are

$$[A^{-1}]=\frac{1}{(\mathbf{g}\times\mathbf{w})\cdot(\mathbf{g}\times\mathbf{w})}\begin{bmatrix}\mathbf{g}-(\mathbf{g}\cdot\mathbf{w})\mathbf{w} & 0\\ \mathbf{w}-(\mathbf{g}\cdot\mathbf{w})\mathbf{g} & 0\\ \mathbf{g}\times\mathbf{w} & 0\\ (\mathbf{g}\cdot\mathbf{w})\mathbf{g}\times\mathbf{w} & (\mathbf{g}\times\mathbf{w})\cdot(\mathbf{g}\times\mathbf{w})\end{bmatrix} \tag{44}$$

and, using the conditions in Eq. (23),

$$[C^{-1}]=\frac{1}{\mathbf{h}\cdot(\mathbf{g}\times\mathbf{w})}\begin{bmatrix}-\mathbf{g} & 0\\ -\mathbf{w} & 0\\ (\mathbf{h}\cdot(\mathbf{g}\times\mathbf{w}))\mathbf{h} & -\mathbf{g}\cdot\mathbf{w}\\ \vec{0} & 1\end{bmatrix}. \tag{45}$$

We obtain the solutions for the joint variables

$$\begin{aligned}\sin\frac{\theta}{2}\cos\frac{\phi}{2}&=\frac{\mathbf{g}\cdot\mathbf{p}-\mathbf{g}\cdot\mathbf{w}\mathbf{w}\cdot\mathbf{p}}{(\mathbf{g}\times\mathbf{w})\cdot(\mathbf{g}\times\mathbf{w})}\\ \cos\frac{\theta}{2}\sin\frac{\phi}{2}&=\frac{\mathbf{w}\cdot\mathbf{p}-\mathbf{g}\cdot\mathbf{w}\mathbf{g}\cdot\mathbf{p}}{(\mathbf{g}\times\mathbf{w})\cdot(\mathbf{g}\times\mathbf{w})}\\ \sin\frac{\theta}{2}\sin\frac{\phi}{2}&=\frac{\mathbf{p}\cdot(\mathbf{g}\times\mathbf{w})}{(\mathbf{g}\times\mathbf{w})\cdot(\mathbf{g}\times\mathbf{w})}\\ \cos\frac{\theta}{2}\cos\frac{\phi}{2}&=\frac{\mathbf{p}\cdot(\mathbf{g}\times\mathbf{w})(\mathbf{g}\cdot\mathbf{w})}{(\mathbf{g}\times\mathbf{w})\cdot(\mathbf{g}\times\mathbf{w})}+p_w,\end{aligned} \tag{46}$$

Table 9 The joint axes for the RPC robots

Joint Axis	*Direction*	*Moment*
G	(−0.42, −0.48, 0.77)	(3.52, −0.36, 1.73)
h	(0.29, −0.87, −0.39)	
W	(−0.92, −0.36, 0.12)	(0.25, −0.05, 1.78)
G	(0.20, −0.43, 0.88)	(0.07, 1.18, 0.55)
h	(0.44, −0.76, −0.47)	
W	(−0.37, −0.63, 0.68)	(0.10, 0.32, 0.36)
G	$(-0.61-0.23i,-0.14-0.01i,0.83-0.17i)$	$(0.16+2.22i,-1.54-2.93i,-0.93+0.96i)$
h	$(-0.55-0.21i,0.94-0.17i,-0.11-0.35i)$	
W	$(-0.17-0.71i,0.24+0.021i,1.19-0.11i)$	$(0.69-0.81i,-1.45-5.57i,0.64+1.49i)$
G	$(-0.61+0.23i,-0.14+0.01i,0.83+0.17i)$	$(0.16-2.22i,-1.54+2.93i,-0.93-0.96i)$
h	$(-0.55+0.21i,0.94+0.17i,-0.11+0.35i)$	
W	$(-0.17+0.71i,0.24-0.021i,1.19+0.11i)$	$(0.69+0.81i,-1.45+5.57i,0.64-1.49i)$
G	$(1.55-1.10i,-1.62-1.57i,0.83-1.01i)$	$(25.09+11.74i,11.63-23.31i,7.64-2.65i)$
h	$(0.35-0.82i,-0.84+0.20i,-1.04-0.44i)$	
W	$(-0.12-0.97i,-1.51+0.02i,0.14-0.61i)$	$(6.49-1.83i,-2.16-5.07i,2.09-1.81i)$
G	$(1.55+1.10i,-1.62+1.57i,0.83+1.01i)$	$(25.09-11.74i,11.63+23.31i,7.64+2.65i)$
h	$(0.35+0.82i,-0.84-0.20i,-1.04+0.44i)$	
W	$(-0.12+0.97i,-1.51-0.02i,0.14+0.61i)$	$(6.49+1.83i,-2.16+5.07i,2.09+1.81i)$

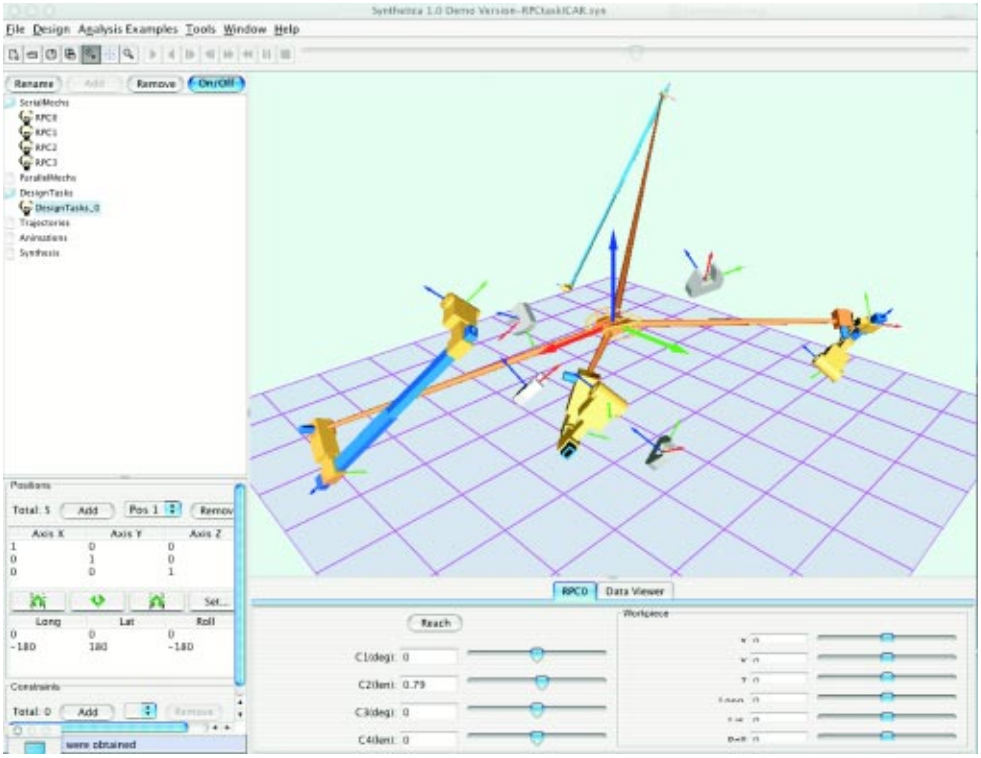

Fig. 8 Four RPC solutions for a 5-position synthesis problem

and

$$\frac{d}{2}\cos\frac{\theta}{2}\sin\frac{\phi}{2}=\frac{b}{2}\left(\frac{(p_w\mathbf{g}\cdot\mathbf{w}-\mathbf{g}\times\mathbf{w}\cdot\mathbf{p})}{\mathbf{h}\cdot\mathbf{g}\times\mathbf{w}}\right)+\frac{\mathbf{g}\cdot\mathbf{w}^0(\mathbf{w}\cdot\mathbf{p}-\mathbf{g}\cdot\mathbf{w}\mathbf{g}\cdot\mathbf{p})-\mathbf{g}^0\cdot\mathbf{g}\times\mathbf{w}\mathbf{p}\cdot\mathbf{g}\times\mathbf{w}-\mathbf{g}\cdot\mathbf{p}^0(\mathbf{g}\times\mathbf{w}\cdot\mathbf{g}\times\mathbf{w})}{\mathbf{h}\cdot\mathbf{g}\times\mathbf{w}(\mathbf{g}\times\mathbf{w}\cdot\mathbf{g}\times\mathbf{w})}$$

$$\frac{d}{2}\sin\frac{\theta}{2}\cos\frac{\phi}{2}=\frac{b}{2}\left(\frac{p_w}{\mathbf{h}\cdot\mathbf{g}\times\mathbf{w}}\right)+\frac{\mathbf{g}^0\cdot\mathbf{w}(\mathbf{g}\cdot\mathbf{p}-\mathbf{g}\cdot\mathbf{w}\mathbf{w}\cdot\mathbf{p})-\mathbf{w}^0\cdot\mathbf{g}\times\mathbf{w}\mathbf{p}\cdot\mathbf{g}\times\mathbf{w}-\mathbf{w}\cdot\mathbf{p}^0(\mathbf{g}\times\mathbf{w}\cdot\mathbf{g}\times\mathbf{w})}{\mathbf{h}\cdot\mathbf{g}\times\mathbf{w}(\mathbf{g}\times\mathbf{w}\cdot\mathbf{g}\times\mathbf{w})}$$

$$\frac{d}{2}\cos\frac{\theta}{2}\cos\frac{\phi}{2}=\frac{b}{2}\left(\frac{-\mathbf{g}\cdot\mathbf{p}\mathbf{h}\cdot\mathbf{g}\times\mathbf{w}}{\mathbf{g}\times\mathbf{w}\cdot\mathbf{g}\times\mathbf{w}}\right)-\frac{\mathbf{g}\cdot\mathbf{w}p_{w0}}{\mathbf{h}\cdot\mathbf{g}\times\mathbf{w}}+\frac{\mathbf{g}\cdot\mathbf{p}(\mathbf{g}\cdot\mathbf{w}\mathbf{h}\cdot\mathbf{w}^0-\mathbf{h}\cdot\mathbf{g}^0)+\mathbf{w}\cdot\mathbf{p}(\mathbf{g}\cdot\mathbf{w}\mathbf{h}\cdot\mathbf{g}^0-\mathbf{h}\cdot\mathbf{w}^0)+(\mathbf{g}\times\mathbf{w}\cdot\mathbf{g}\times\mathbf{w})\mathbf{h}\cdot\mathbf{p}^0}{\mathbf{g}\times\mathbf{w}\cdot\mathbf{g}\times\mathbf{w}}$$

$$\frac{d}{2}\sin\frac{\theta}{2}\sin\frac{\phi}{2}=\frac{b}{2}\left(\frac{\mathbf{w}\cdot\mathbf{p}}{\mathbf{h}\cdot\mathbf{g}\times\mathbf{w}}\right)+\frac{\mathbf{p}\cdot\mathbf{g}\times\mathbf{w}(\mathbf{g}^0\cdot\mathbf{w}+\mathbf{g}\cdot\mathbf{w}^0)+p_{w0}(\mathbf{g}\times\mathbf{w}\cdot\mathbf{g}\times\mathbf{w})}{\mathbf{h}\cdot\mathbf{g}\times\mathbf{w}(\mathbf{g}\times\mathbf{w}\cdot\mathbf{g}\times\mathbf{w})}. \tag{47}$$

When using the relation between the variables of Eq. (46), and simplifying the extra factors, we obtain a design equation without joint variables. This equation can be expanded to

$$\begin{aligned}R_1:\quad & g_x((-p_y^2-p_z^2)w_x+(p_xp_y-p_wp_z)w_y+(p_wp_y+p_xp_z)w_z)\\ & +g_y((p_xp_y+p_wp_z)w_x+(-p_x^2-p_z^2)w_y+(p_yp_z-p_wp_x)w_z)\\ & +g_z((p_xp_z-p_wp_y)w_x+(p_wp_x+p_yp_z)w_y+(-p_x^2-p_y^2)w_z)\\ & =0\end{aligned} \tag{48}$$

References

[1] Schoenflies, A., 1886, *Geometrie der Bewegung in Synthetischer Darstellung*, Leipzig, Germany. (See also the French translation: *La Géométrie du Movement*, Paris, 1983.)
[2] Burmester, L., 1886, *Lehrbuch der Kinematik*, Verlag Von Arthur Felix, Leipzig, Germany.
[3] Roth, B., 1967, "Finite Position Theory Applied to Mechanism Synthesis," ASME J. Appl. Mech., **34E**, pp. 599–605.
[4] Hartenberg, R., and Denavit, J., 1964, *Kinematic Synthesis of Linkages*, McGraw-Hill, New York, NY.
[5] Sandor, G. N., and Erdman, A. G., 1984, *Advanced Mechanism Design: Analysis and Synthesis*, Vol. 2. Prentice-Hall, Englewood Cliffs, NJ.
[6] Suh, C. H., and Radcliffe, C. W., 1978, *Kinematics and Mechanisms Design*, John Wiley & Sons, New York.
[7] McCarthy, J. M., 2000, *Geometric Design of Linkages*, Springer-Verlag, New York.
[8] Hunt, K. H., 1978, *Kinematic Geometry of Mechanisms*, Clarendon Press.
[9] Suh, C. H., 1968, "Design of Space Mechanisms for Rigid-Body Guidance," ASME J. Ind., **90B**, pp. 499–506.
[10] McCarthy, J. M., 1995, "The Synthesis of Planar RR and Spatial CC Chains and the Equation of a Triangle," ASME J. Mech. Des., **117**(B), pp. 101–106.
[11] Huang, C., and Chang, Y-J., 2000, "Polynomial Solution to the Five-Position Synthesis of Spatial C-C Dyads via Dialytic Elimination," *Proc. ASME Design*

Engineering Technical Conference, Paper No. DETC2000/MECH-14102, Baltimore, Maryland, Sept. 10–13.
[12] Kihonge, J. N., Vance, J. M., and Larochelle, P. M., 2002, ''Spatial Mechanism Design in Virtual Reality with Networking,'' ASME J. Mech. Des., **124**(**3**), pp. 435–440.
[13] Innocenti, C., 1995, ''Polynomial Solution of the Spatial Burmester Problem,'' ASME J. Mech. Des., **117**(1).
[14] Liao, Q., and McCarthy, J. M., 2001, ''On the Seven Position Synthesis of a 5-SS Platform Linkage,'' ASME J. Mech. Des., **123**(1), pp. 74–79.
[15] Chen, P., and Roth, B., 1967, ''Design Equations for Finitely and Infinitesimally Separated Position Synthesis of Binary Link and Combined Link Chains,'' ASME J. Ind., **91**, pp. 209–219.
[16] Nielsen, J., and Roth, B., 1995, ''Elimination Methods for Spatial Synthesis,'' Computational Kinematics, J. P. Merlet and B. Ravani eds., Vol. 40 of *Solid Mechanics and Its Applications*, pp. 51–62, Kluwer Academic Publishers.
[17] Kim, H. S., and Tsai, L. W., 2003, ''Kinematic Synthesis of Spatial 3-RPS Parallel Manipulators,'' ASME J. Mech. Des., **125**(1), pp. 92–97.
[18] Tsai, L. W., and Roth, B., 1972, ''Design of Dyads with Helical, Cylindrical, Spherical, Revolute and Prismatic Joints,'' Mech. Mach. Theory, **7**, pp. 591–598.
[19] Tsai, L. W., 1972, ''Design of Open Loop Chains for Rigid Body Guidance,'' Ph.D. Thesis, Department of Mechanical Engineering, Stanford University.
[20] Tsai, L. W., and Roth, B., 1973, ''A Note on the Design of Revolute-Revolute Cranks,'' Mech. Mach. Theory, **8**, pp. 23–31.
[21] Perez, A., and McCarthy, J. M., 2000, ''Dimensional Synthesis of Bennett Linkages,'' Proc. 2000 ASME Design Engineering Technical Conferences, Baltimore, MD, Sept. 10–13.
[22] Sandor, G. N., 1968, ''Principles of a General Quaternion-Operator Method of Spatial Kinematic Synthesis,'' ASME J. Appl. Mech., **35**(1), pp. 40–46.
[23] Sandor, G. N., and Bisshopp, K. E., 1969, ''On a General Method of Spatial Kinematic Synthesis by Means of a Stretch-Rotation Tensor,'' ASME J. Ind., **91**, pp. 115–122.
[24] Sandor, G. N., Weng, T. C., and Xu, Y., 1988, ''The Synthesis of Spatial Motion Generators With Prismatic, Revolute and Cylindric Pairs Without Branching Defect,'' Mech. Mach. Theory, **23**(4), pp. 69–274.
[25] Sandor, G. N., Xu, Y., and Weng, T. C., 1986, ''Synthesis of 7-R Spatial Motion Generators with Prescribed Crank Rotations and Elimination of Branching,'' Int. J. Robot. Res., **5**(2), pp. 143–156.
[26] Mavroidis, C., Lee, E., and Alam, M., 2001, ''A New Polynomial Solution to the Geometric Design Problem of Spatial RR Robot Manipulators Using the Denavit-Hartenberg Parameters,'' ASME J. Mech. Des., **123**(1), pp. 58–67.
[27] Lee, E., Mavroidis, C., and Merlet, J. P., 2002, ''Five Precision Points Synthesis of Spatial RRR Manipulators Using Interval Analysis,'' *Proc. ASME 2002 Design Eng. Tech. Conf.*, paper no. DETC2002/MECH-34272, Sept. 29-Oct. 2, Montreal, Canada.
[28] Lee, E., and Mavroidis, D., 2002, ''Solving the Geometric Design Problem of Spatial 3R Robot Manipulators Using Polynomial Homotopy Continuation,'' ASME J. Mech. Des., **124**(4), pp. 652–661.
[29] Lee, E., and Mavroidis, D., 2002, ''Geometric Design of Spatial PRR Manipulators Using Polynomial Elimination Techniques,'' *Proc. ASME 2002 Design Eng. Tech. Conf.*, paper no. DETC2002/MECH-34314, Sept. 29-Oct. 2, Montreal, Canada.
[30] Gupta, K. C., 1986, ''Kinematic Analysis of Manipulators Using Zero Reference Position Description,'' Int. J. Robot. Res., **5**(2), pp. 5–13.
[31] Tsai, L. W., 1999, *Robot Analysis: The Mechanics of Serial and Parallel Manipulators*, John Wiley and Sons, New York, NY.
[32] Yang, A. T., and Freudenstein, F., 1964, ''Application of Dual-Number Quaternion Algebra to the Analysis of Spatial Mechanisms,'' ASME J. Appl. Mech., June, pp. 300–308.
[33] McCarthy, J. M., 1990, *Introduction to Theoretical Kinematics*, The MIT Press, Cambridge, MA.
[34] Shoham, M., and Jen, F. H., 1994, ''On Rotations and Translations with Application to Robot Manipulators,'' Advanced Robotics, **8**(2), pp. 203–229.
[35] Angeles, J., 1998, ''The Application on Dual Algebra to Kinematic Analysis,'' *Computational Methods in Mechanical Systems*, NATO ASI Series, J. Angeles and E. Zakhariev, eds., Springer, Berlin.
[36] Ravani, B., and Ge Q. J., 1991, ''Kinematic Localization for World Model Calibration in Off-Line Robot Programming Using Clifford Algebra,'' *Proc. of IEEE International Conf. on Robotics and Automation*, Sacramento, CA, April, pp. 584–589.
[37] Larochelle, P., 2000, ''Approximate Motion Synthesis via Parametric Constraint Manifold Fitting,'' *Advances in Robot Kinematics*, J. Lenarcic and M. M. Stanisic, eds., Kluwer Acad. Publ., Dordrecht.
[38] Perez, A., and McCarthy, J. M., 2002, ''Dual Quaternion Synthesis of Constrained Robots,'' *Advances in Robot Kinematics*, J. Lenarcic and F. Thomas, eds., Kluwer Academic Publ. 443–454. Caldes de Malavella, Spain, June 24–29.
[39] Craig, J. J., 1989, *Introduction to Robotics, Mechanics and Control*, Addison Wesley Publ. Co, Reading, MA.
[40] Bottema, O., and Roth, B., 1979, *Theoretical Kinematics*, North Holland Press, NY.
[41] Perez, A., 2003, ''Dual Quaternion Synthesis of Constrained Robotic Systems,'' Ph.D. Thesis, Department of Mechanical Engineering, University of California, Irvine.
[42] Verschelde, J., 1999, ''Algorithm 795: PHCpack: A Generalpurpose Solver for Polynomial Systems by Homotopy Continuation,'' ACM Trans. Math. Softw., **25**(2), 251276, 1999. Software available at http://www.math.uic.edu/jan.
[43] Su, H., Collins, C., and McCarthy, J. M., ''An Extensible Java Applet for Spatial Linkage Synthesis,'' *Proc. ASME Des, Eng. Technical Conferences*, paper no. DETC2002/MECH-24271, Montreal, Canada, 2002.
[44] Collins, C., McCarthy, J. M., Perez, A., and Su, H., 2002, ''The Structure of an Extensible Java Applet for Spatial Linkage Synthesis,'' ASME J. Computing and Information Science in Engineering, **2**(1), pp. 45–49.